MICROSTRUCTURAL INHOMOGENEITIES IN V-4Cr-4Ti MECHANICAL PROPERTY SPECIMENS PREPARED FOR IRRADIATION EXPERIMENTS IN HFBR, BOR-60, AND HFIR – A. F. Rowcliffe and D. T. Hoelzer (Oak Ridge National Laboratory)

SUMMARY

Significant variations exist between the microstructures of the various batches of mechanical property specimens prepared for the 500 kg heat of V-4Cr-4Ti. The development of banded grain structures is shown to be related to non-homogeneous distribution of Ti (OCN) particles (0.1-0.3 μ in diameter) that occur in some, but not all, plate products. Precipitation of Ti (OCN) will occur during the hot extrusion of the ingot in regions where the dislocation density is high and where the temperature falls below the Ti (OCN) solvus at 1125°C. Investigation of the potential benefits of a homogenizing treatment at 1150°C is recommended before proceeding with additional fabrication of plate products from the extruded bar.

PROGRESS AND STATUS

Introduction

Beginning at the end of 1994, a series of sheet and plate materials prepared from the 500 kg heat of V-4Cr-4Ti (heat No. 832665) were supplied to ORNL from Teledyne Wah-Chang, Albany (TWCA) via ANL. These batches have been used to prepare a series of SS-3 tensile specimens and one-third-size Charpy Vee-Notch (CVN) specimens for unirradiated measurements and for irradiated testing.

Variations in the processing and manufacturing conditions have resulted in small differences in final microstructure between various batches and recently it has been observed [1] that there are significant differences in fracture behavior between different batches of CVN specimens. This report: (a) summarizes the fabrication histories of the various starting materials and specimens; (b) characterizes the microstructural differences between the various batches; and (c) seeks to understand the origins of the observed microstructural inhomogeneities.

RESULTS

Table 1 summarizes the identification codes, dimensions, and metallurgical condition of plate and sheet stock supplied by TWCA via ANL. Table 2 summarizes the specimen identification codes used by ORNL researchers in various irradiation experiments. The SS-3 specimens were prepared in four separate campaigns from three different initial batches of plate-stock, as described in Table 3. The CVN specimens were prepared in four separate campaigns from three different plates, as described in Table 4.

SS-3 Tensile Specimens

A summary of physical and mechanical properties of the four batches of SS-3 tensiles is shown in Table 5 (specimens labeled RC or RD are from the same batch of material). Although the tensile specimens came from different plates and were subjected to different final processing steps, significant differences in hardness and resistivity could not be detected. However, there were some small but significant differences in RT yield strength; the ST and RC/D series being stronger by 20 to 25 MPa than the WH and WE series tensile specimens.

Table 1: Identification of Plate and Sheet Stock of V-4Cr-4Ti (832665)

ANL I.D.	Date Received	Dimensions (cm)	Thickness (cm)	TWCA Supplied Condition	ORNL I.D.	Experimental Use
Plate B	8/94	9.5 × 10	0.38	Ann. 1050°C/2h	L150	WA series CVN
Plate A	9/94	18.5 × 23.5	0.38	Ann. 1050°C/2h	M150	WB series CVN
Plate D	9/94	24 × 26.5	0.10	~50% CW	N40	WE, WH series SS-3
Plate C	9/94	16.5 × 33	0.64	Ann. 1050°C/2h	P250	Welding
Plate A Ann.	5/95	14 × 30	0.64	Ann. 1050°C/2h	Q250	QC series CVN
–	10/95	17 × 18	0.64	Ann. 1050°C/2h	–	Welding
–	10/95	19.5 × 20	0.10	~50% CW	–	–
–	2/96	23 × 39	0.64	Ann. 1000°C/1h	R250A	Welding
–	2/96	23 × 39	0.64	~50% CW	R250	RC series CVN, SS-3
–	2/96	23 × 39	0.38	~50% CW	T150	–
–	2/96	24 × 36.5	0.10	~50% CW	S40	ST series SS-3
Plate DD	8/98	20 × 39	0.38	~50% CW	V150	–
Plate D	8/98	12.5 × 27	0.64	~50% CW	V250	–

Table 2. Identification Codes for V-4Cr-4Ti (832665) Irradiation Specimens

Irradiation Experiment	I.D. Codes SS-3	I.D. Codes CVN	I.D. Codes DCT
HFBR-V1	WH 01-03	WB 83-151	–
HFBR-V2	WH 08-14	WB 78-159	–
HFBR-V3	WH 23-25 ST 12-44	QC 95-199	–
HFBR-V4	ST 53-75	QC 113-202	–
ATR-A1	–	QC 01-10	QA 05-06
BOR-60 (Fusion 1)	WE 01-12 WE 21-25	WB 32-77	WC 01-18
HFIR-RB-10J	RC 06-47	RC 11-97	RC 01-03

Table 3. Processing Histories for SS-3 Tensile Specimens

ST Series	WH Series	WE Series	RC/D Series
Plate S40 1.02 mm thick ~50% CR ↓ Machined specimens ↓ Vac. ann. 1000°C, 2h	Plate N40 1.02 mm thick ~50% CR ↓ Machined specimens ↓ Vac. ann. 1000°C, 2h	Plate N40 1.02 mm thick ~50% CR ↓ Vac. ann. 950°C, 2h ↓ 50% CR to 0.76 mm thick ↓ Machined specimens ↓ Vac. ann. 1000 or 1050°C, 2h	Plate R250 ↓ Vac. ann. 1000°C, 2h ↓ 40% cross-rolled to 3.8 mm thick in 10 passes ↓ ORNL I.D.: R150 ↓ Machined specimens ↓ Vac. ann. 1000°C, 2h

Table 4. Processing Histories for CVN Specimens

WB Series	QC (01-40)	QC (41-210)	RC Series
Plate M150 3.8 mm thick 1050°C, 2h (TWCA) ↓ Machined specimens (LT orientation) ↓ Vac. ann. 1000°C, 2h	Plate Q250 6.4 mm thick 1050°C, 2h (TWCA) ↓ Machined specimens (LT orientation) ↓ Vac. ann. 1000°C, 2h	Plate Q250 6.4 mm thick 1050°C, 2h (TWCA) ↓ 40% cross-rolled to 3.8 mm thick in 10 passes ↓ Machined specimens (LT orientation) ↓ Vac. ann. 1000°C, 2h	Plate R250 6.4 mm thick 50% CR (TWCA) ↓ Vac. ann. 1000°C, 2h ↓ 40% cross-rolled to 3.8 mm thick in 10 passes ↓ Machined specimens (LT orientation ↓ Vac. ann. 1000°C, 2h

*LT orientation in each case is with respect to the cold-rolling direction of the TWCA plate.

Table 5. Average Physical and Mechanical Properties of SS-3 Specimens Following Final Anneal (1000°C, 2h)

SS-3 Series	Grain Size ±2 μm	Hardness ±5 VHN	RT Yield ±10 MPa	Resistivity ±0.6 n Ω-m
ST	15	140	356	283.7
WH	26	134	330	280.3
WE	12/40 banded	141	334	281.4
RC/D	23	137	356	281.9

There are significant differences in grain size and in microstructural homogeneity between the batches. The ST and WH series of tensiles were machined directly from the cold-worked plates S40 and N40, followed by final annealing at 1000°C/2h. The microstructure of both batches are fairly homogeneous, with grains slightly elongated in the rolling direction (Fig. 1a and b). The average grain size of the WH series (~26 μ) is significantly larger than that of the ST series (~15 μ), probably as a result of differing final levels of CW in the two plates. On the other hand, the microstructure of the WE series is relatively inhomogeneous (Fig. 2a, b, and c), with bands of coarse grains (~40 μ dia) interspersed with regions of finer grains (15-20 μ dia). The finer grains are associated with bands of Ti (OCN) particles aligned along the rolling direction of the plate. In contrast, the microstructure of the RC/D series (Fig. 1c) is uniform, with a more uniaxed grain structure than the other three series, presumably as a result of the 40% cross-rolling treatment prior to the final anneal (Table 3).

CVN Specimens

The CVN specimens used in the HFBR, BOR-60, ATR, and HFIR irradiation experiments were fabricated in four campaigns, as shown in Table 4. In each campaign, the specimens were machined in an L-T orientation with respect to the rolling direction marked on the plate material received from TWCA. The WB series and the WC (01-40) specimens were machined directly from the TWCA annealed plate. On the other hand, the CVN specimens with ID numbers QC (41-20) and the RC series were machined from plates which had been 40% cold-rolled at ORNL in a direction perpendicular to the TWCA rolling direction.

QC Series

Both sets of specimens (01-40) and (41-210) originated from plate Q250 and both sets are characterized by dispersions of Ti (OCN) particles unevenly distributed in bands throughout the microstructure. The bands of particles are typically 200-300 μ wide in the transverse plate direction (T), around 20-100 μ thick in the short plate direction (S), and almost continuous in the longitudinal or rolling direction (L) [Figs. 3 and 4]. Within the precipitate rich regions, grain growth is restricted and a microstructure of alternating bands of coarse (30-50 μ dia) and fine (10-20 μ dia) grains develops during the final recrystallization treatment at 1000°C. The Ti (OCN) particles are believed to develop during the hot extrusion of the cast billet and to persist during subsequent cold rolling and annealing operations, as discussed below. The banded nature of the grain structure is less pronounced in the QC (41-210) series of specimens (Fig. 4) than in the QC (01-40) series (Fig. 3); as a result of differences in processing history (Table 4). Before machining the QC (41-210) series, the 6.4 mm plate was cold-rolled 40% in a direction perpendicular to the TWCA rolling direction. The cross-rolled material subsequently develops a more equiaxed and less banded grain structure during the final recrystallization treatment at 1000°C. The QC (01-40) series, on the other hand, were machined directly from the annealed plates supplied by TWCA, and the post-machining anneal at 1000°C only served to remove any hydrogen picked-up during machining and did not affect the microstructure.

WB Series

This set of specimens originated from the TWCA annealed plate M150 and the microstructure is very similar to that of the QC (01-40) specimens, with the characteristic banded grain distribution associated with a non-uniform dispersion of Ti (OCN) [Fig. 5]. The distribution of particles within a band is shown in Fib. 5b in an LS section and in Fig. 5c in an LT section.

1(a)

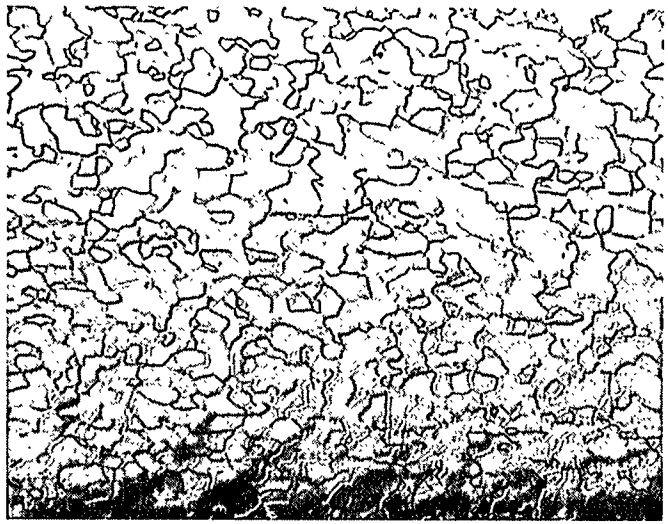

1(b)

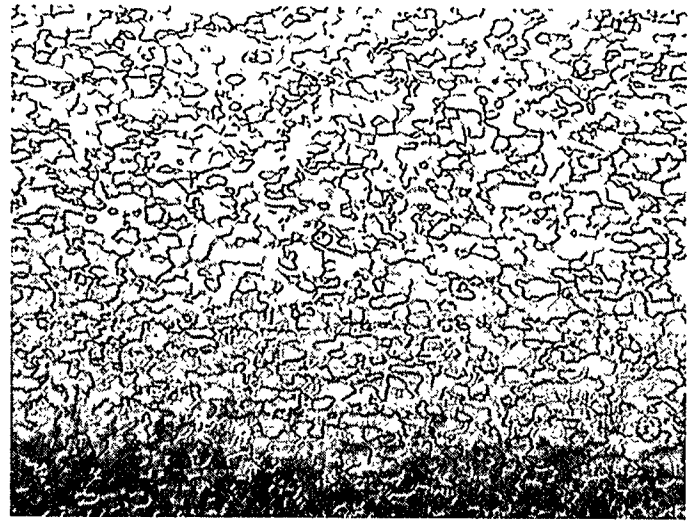

100X 50μm

1(c)

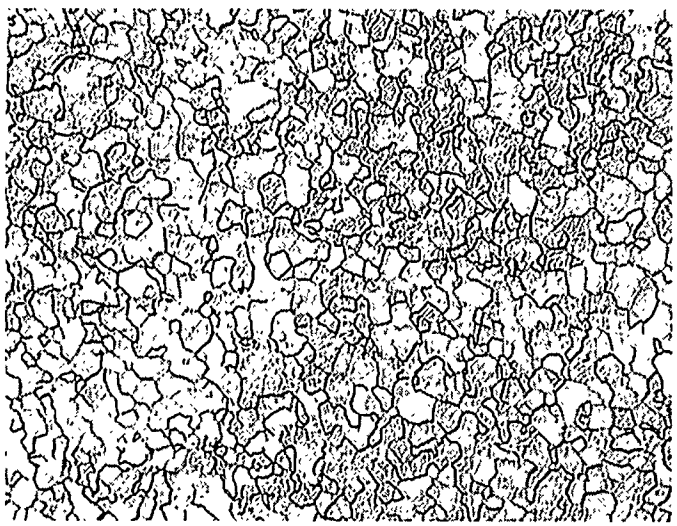

Fig. 1. Optical microstructures of 3 batches of SS-3 tensile specimens: (a) WH series, (b) ST series, and (c) RC/D series. The WH and ST series have a grain structure slightly elongated in the plate rolling direction; the RC/D series has an equi-axed grain structure.

2(a)

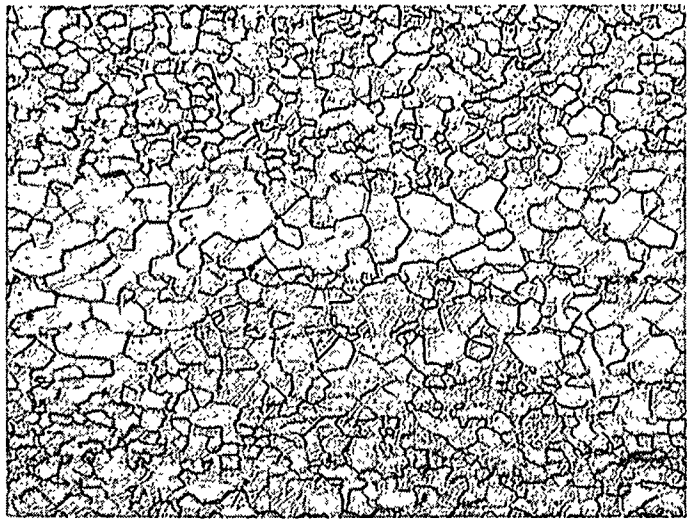

2(b)

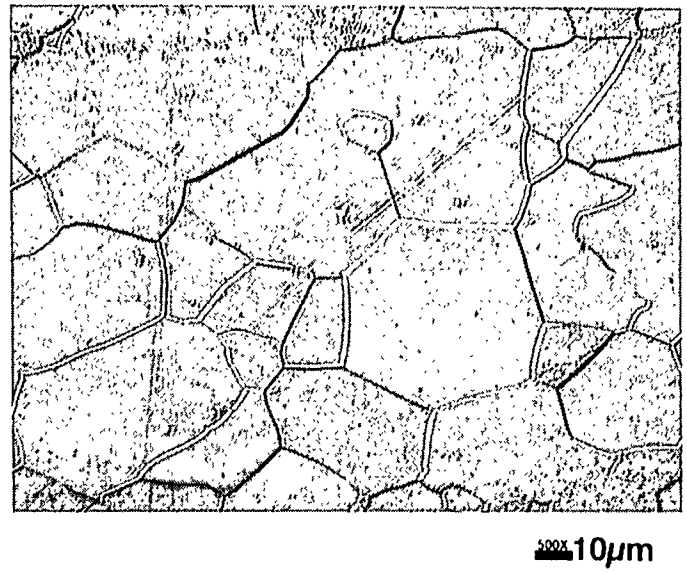

2(c)

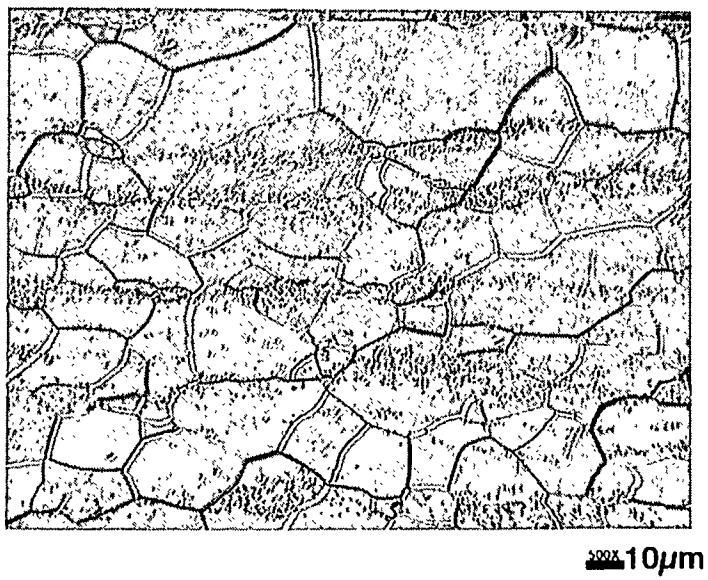

Fig. 2. Optical microstructure of the WE series SS-3 tensile specimens with an inhomogeneous banded distribution of grains (a). Areas with large grains are relatively precipitate-free (b); regions of finer grains are associated with bands of Ti (OCN) particles (c).

3(a)

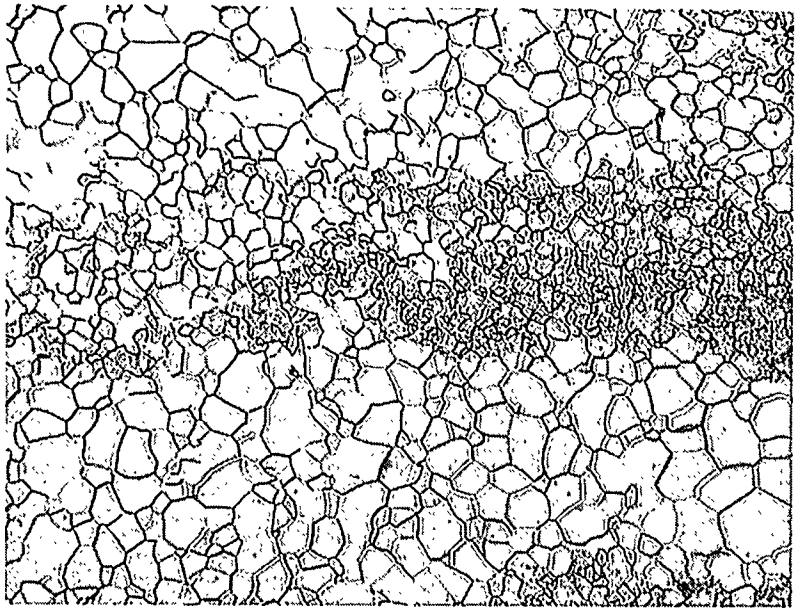

100X 50μm

3(b)

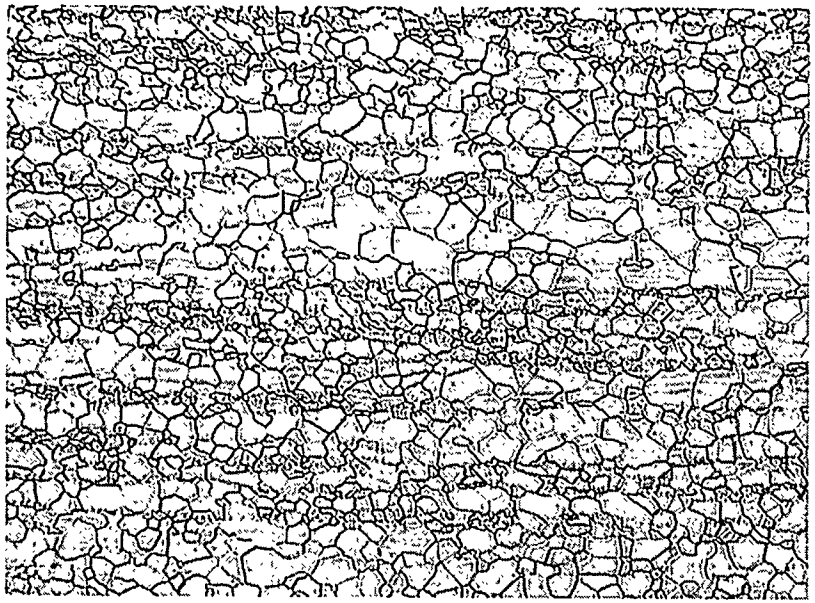

100X 50μm

3(c)

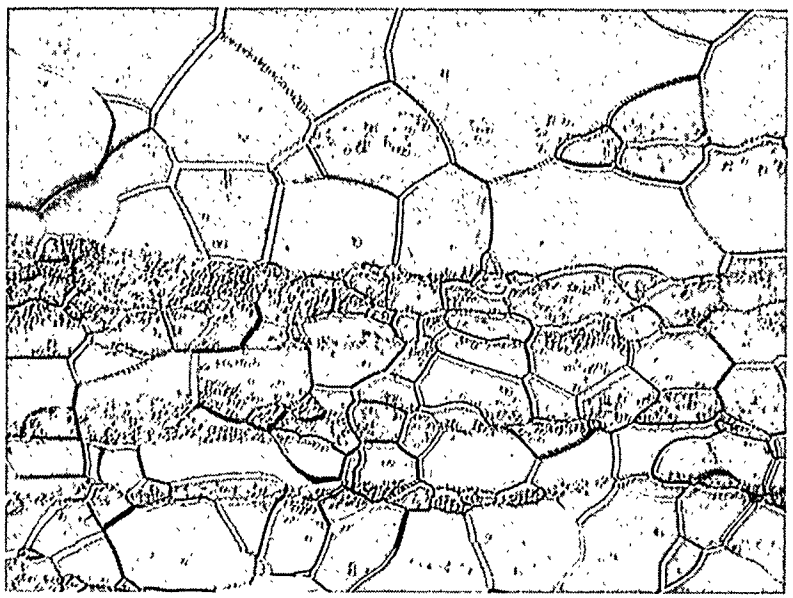

500X 10μm

Fig. 3. Optical microstructure of CVN specimen from the QC (01-40) series showing banded grain structure associated with inhomogeneous distribution of Ti (OCN) particles: (a) LT orientation; (b) and (c) LS orientation.

4(a)

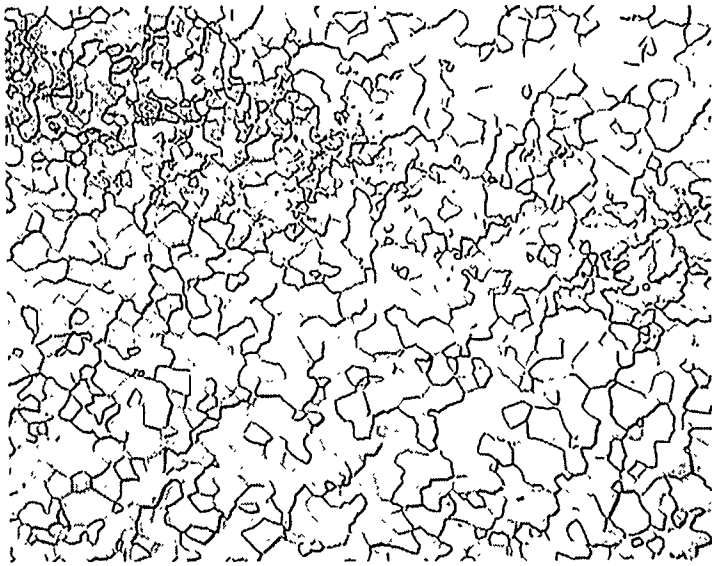

4(b)

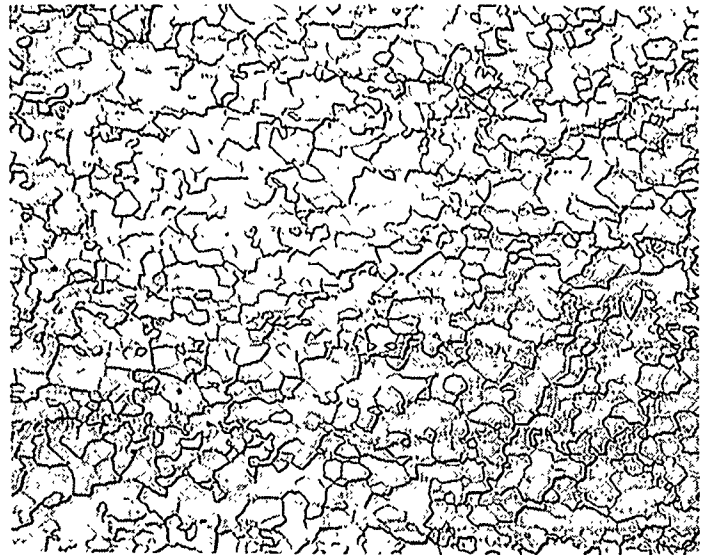

4(c)

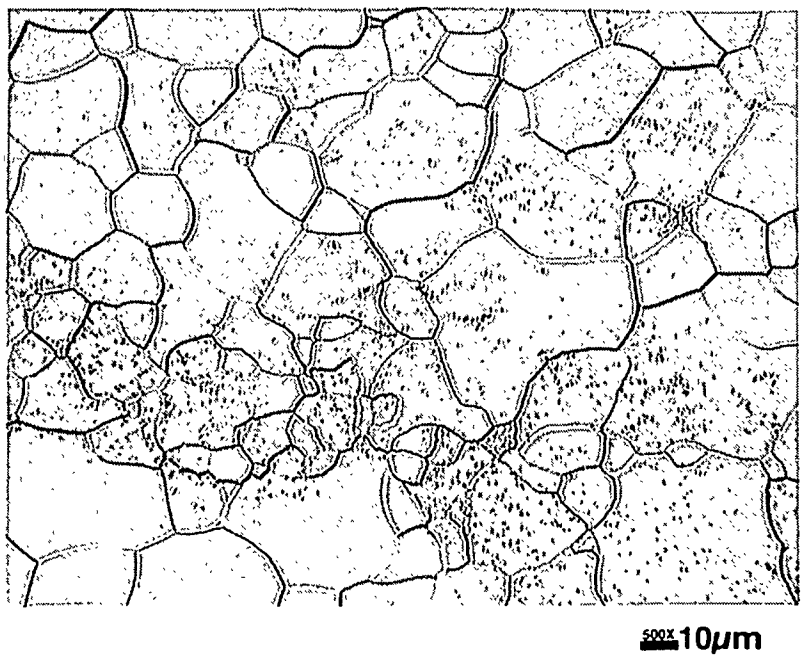

Fig. 4. Optical microstructure of CVN specimen from the QC (41-210) series showing banded grain microstructure associated with inhomogeneous distribution of Ti (OCN) particles: (a) LT orientation; (b) and (c) LS orientation.

5(a)

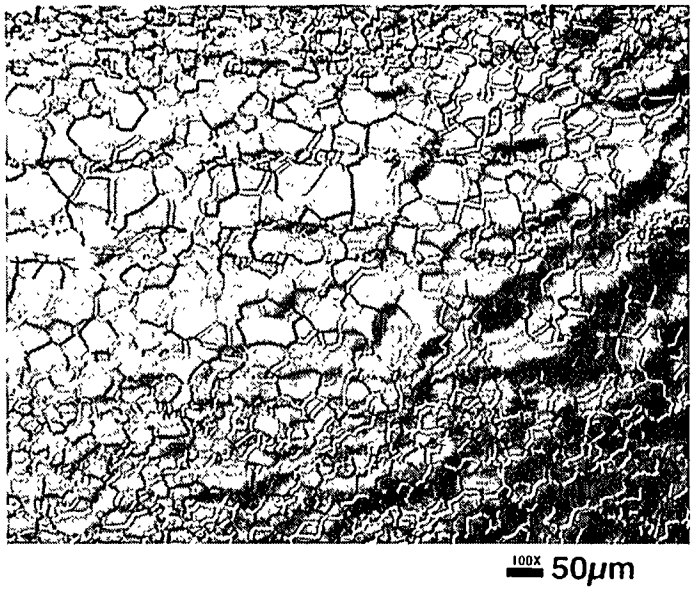

5(b)

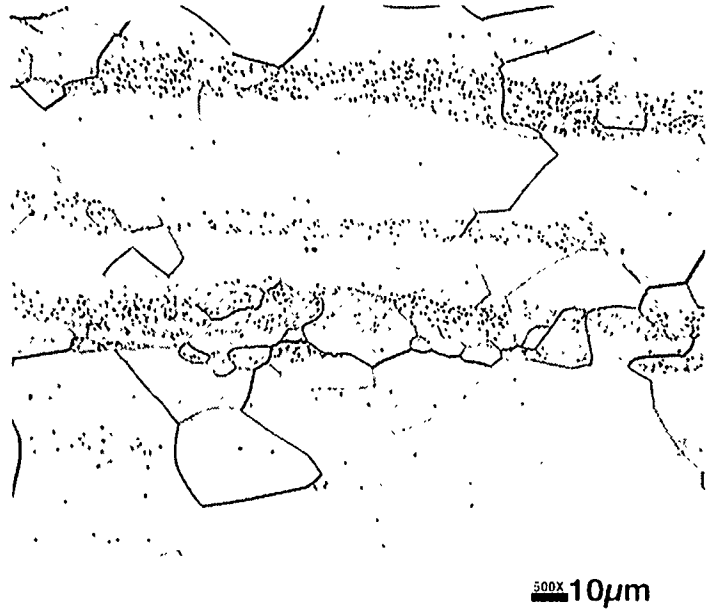

5(c)

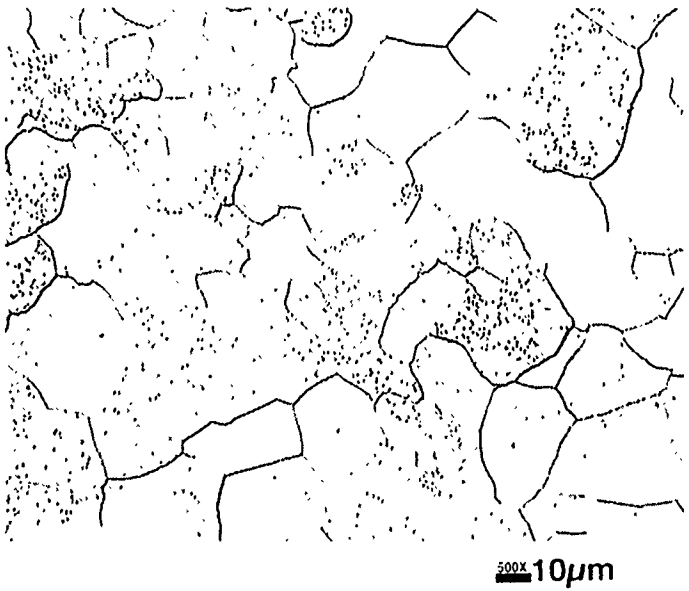

Fig. 5. Optical microstructure of CVN specimen from the WB series showing banded microstructure associated with inhomogeneous distribution of Ti (OCN) particles; (a) and (b) LS orientation; (c) LT orientation.

RC Series

The microstructure of these specimens, which originated from plate R250, is quite different from those of the other three sets that were derived from plates Q250 and M150. As shown in the low magnification micrographs in Fig. 6a and b, the grain structure is uniform (average grain size ~23 μ), with no evidence of the bands of fine grains that characterize the other sets. The TI (OCN) particles, while showing some tendency toward alignment in the rolling direction (Fig. 6c), are much more uniformly dispersed than in the other sets of specimens.

Precipitation of Ti (OCN)

In an accompanying article [2], it is shown that the globular phase referred to as Ti (OCN) is based upon the fcc TiC phase, which accommodates the other interstitials O and N. In an earlier progress report, Kurtz et al. [3] showed with optical microscopy that the volume fraction of globular particles in heat 832665 can be significantly reduced by heat treating at 1125°C for one hour. The coarse particles re-precipitated during a subsequent treatment at 890°C for two hours. This observation indicates that a solvus for the Ti (OCN) phase exists in the vicinity of 1125°C. As further confirmation of this solvus, a CVN specimen with an inhomogeneous banded microstructure (QC30) was heat treated at 1125°C for two hours in a vacuum of 5×10^{-7} torr. Dissolution of the Ti (OCN) occurred, accompanied by rapid grain growth in the regions between the original bands of particles. Within the banded regions, however, particle dissolution was not complete and the finer grain sizes still persisted. This is illustrated in Fig. 7. These micrographs of the specimen heat treated at 1125°C provide a graphic illustration of the inhomogeneous nature of the microstructures derived from plate Q250. To investigate the origins of this inhomogeneity, metallographic samples were prepared from sections taken from an as-extruded bar (6.3 × 6.3 × 50 cm). The extrusion of the 500 kg heat was carried out by sealing a semi-ingot in a stainless steel jacket and heating at 1150°C for three hours before extrusion [4].

The microstructure of the as-extruded material shown in Fig. 8 consists of an inhomogeneous mixture of small grains (20-60 μ), coarse grains (100-150 μ), and elongated deformed regions arranged in bands parallel to the extrusion direction. Examination of six different metallographic specimens failed to produce any evidence of Ti (OCN) precipitation, although the optical technique being used would not detect particles below about 0.1 μ.

During extrusion, non-homogeneous plastic flow patterns develop that depend upon the alloy flow properties, temperature distribution, die friction, and extrusion speed. The thermal situation is complex and temperatures are influenced by heat generation due to plastic deformation, internal shear, friction with the tooling, and the heat transfer within the billet and through the tooling. Typically, the emergent temperature increases with ram displacement, ram speed, and with reduction ratio. The temperature at the product surface is higher than at the product center.

During extrusion of the V-4Cr-4Ti, dynamic recovery and recrystallization occur to an extent that reflects the inhomogeneity of the deformation rate and temperature distribution. At the same time, precipitation of Ti (OCN) will occur whenever the temperature falls below the solvus at ~1125°C. Because of the incoherent nature of the TI (OCN) precipitate-matrix interface, precipitation will occur most rapidly in areas of high dislocation density. Precipitation of Ti (OCN) can occur (a) during hot deformation in regions where the temperature falls below ~1125°C, and, to a lesser extent, (b) in regions of high dislocation density during cool-down of the extrusion.

Because of the inhomogeneous nature of both the deformation and temperature distribution, it is very likely that precipitation of Ti (OCN) will also be distributed non-homogeneously. However, in

6(a)

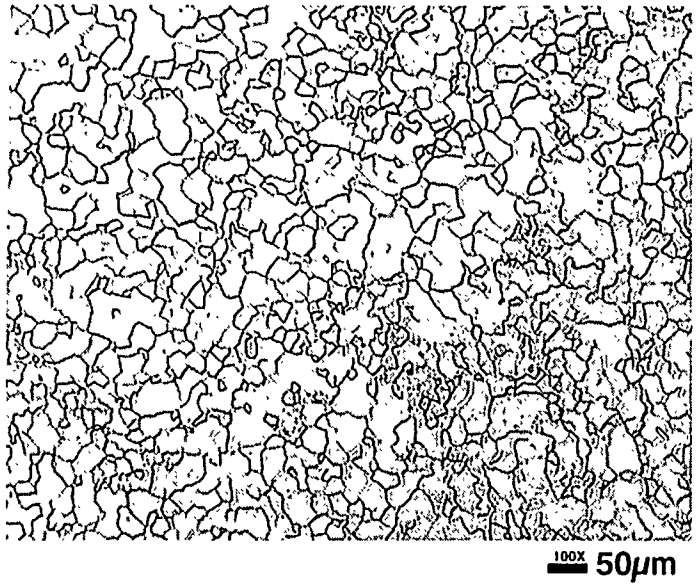

6(b)

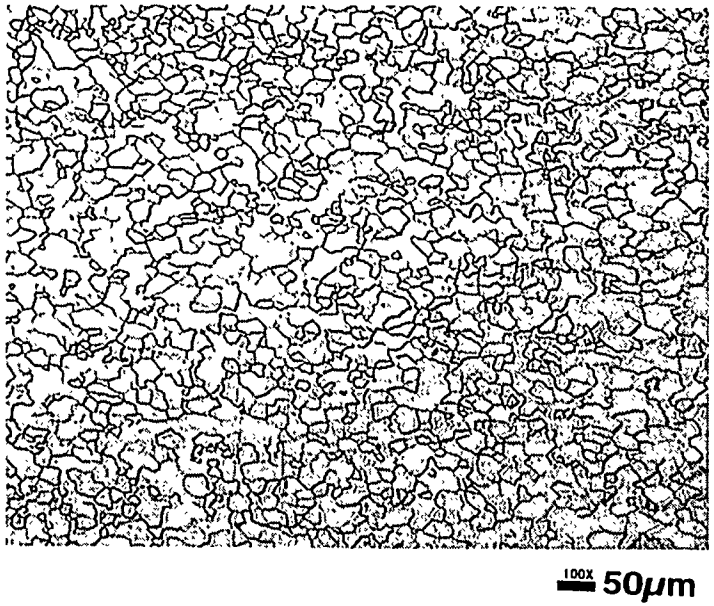

6(c)

Fig. 6. Optical microstructure of CVN specimen from the RC series showing a more uniform distribution of Ti (OCN) particles and absence of banded grain structure: (a) LT orientation; (b) and (c) LS orientation.

7(a)

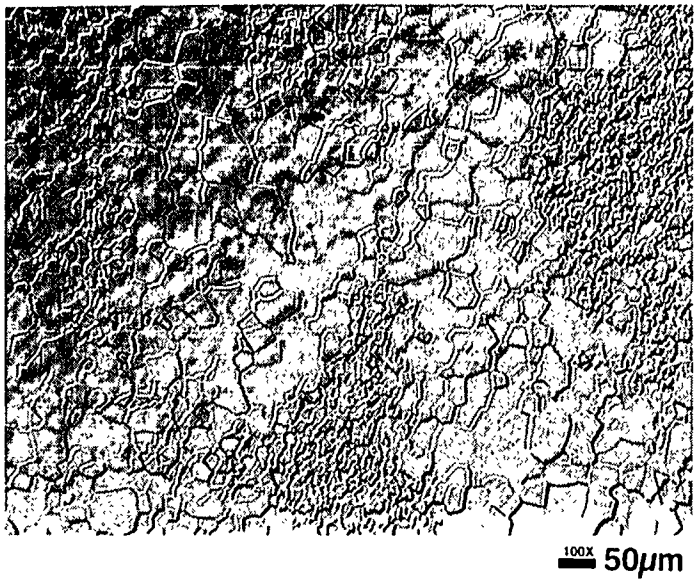

7(b)

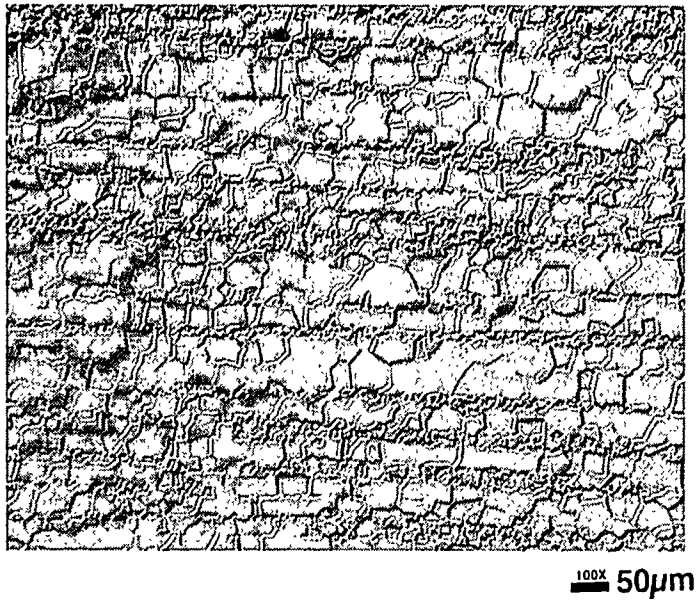

7(c)

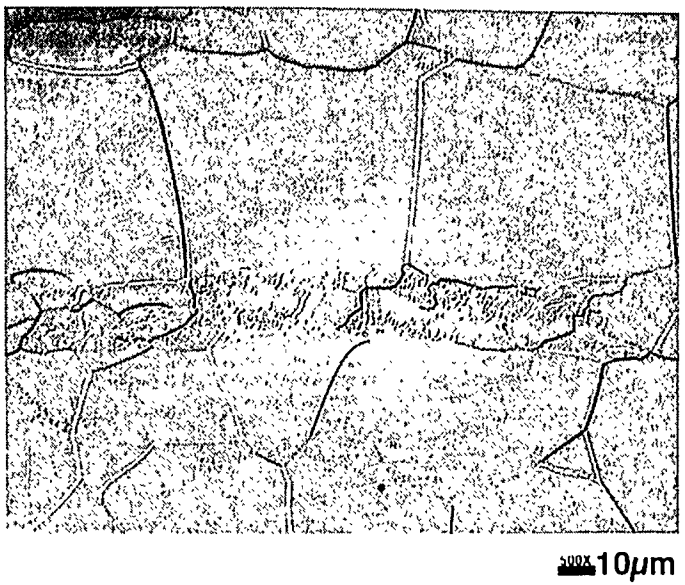

Fig. 7. Optical microstructure of CVN specimen from the QC (01-40) series after heat-treating at 1125°C for 2h, illustrating partial dissolution of Ti (OCN) and grain growth: (a) LT orientation; (b) and (c) LS orientation.

8(a)

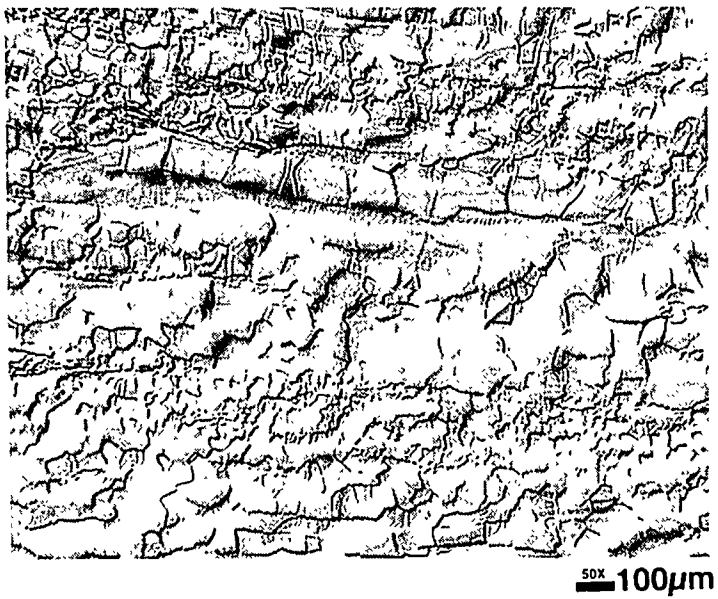

8(b)

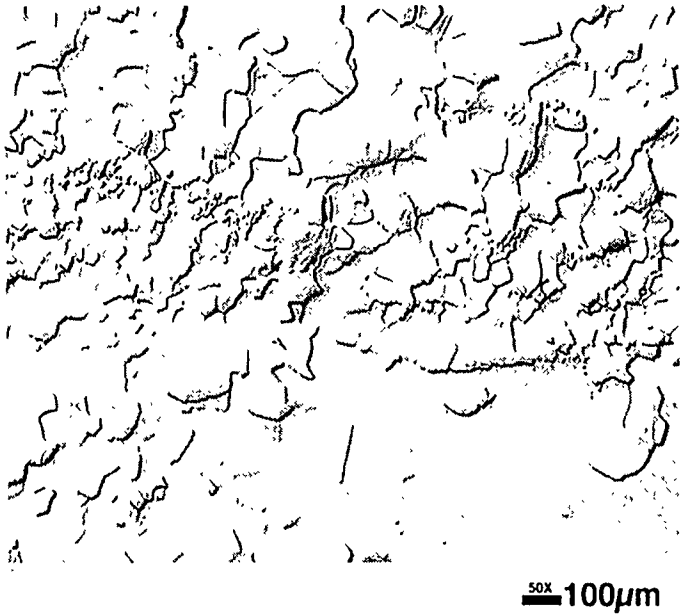

8(c)

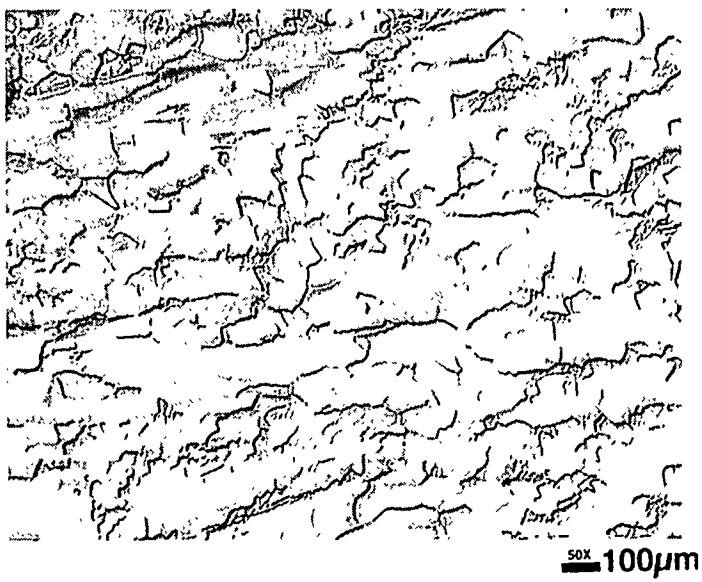

Fig. 8. Optical microstructure of as-extruded V-4Cr-4Ti showing fine equi-axed grains, large elongated grains, and un-recrystallized regions. Sections (a) and (b) are parallel to the extrusion direction, (c) is perpendicular to the extrusion direction.

regions of the billet where the temperature remains above ~1125°C during extrusion, precipitation during deformation will not occur and subsequent precipitation of Ti (OCN) during secondary processing is likely to be much more uniformly dispersed.

Secondary processing consists of rolling to a maximum of 50% reduction at temperatures in the range RT to 400°C with intermediate annealing at 1050 to 1075°C. Since this is below the Ti (OCN) solvus, inhomogeneous distributions of Ti (OCN) developed during extrusion cannot be eliminated. Grain growth is inhibited in regions of high particle density and a banded recrystallized grain structure develops that persists in the final microstructure of the mechanical property specimen. This seems to be the situation with the QC and WB series of CVN specimens and indicates that plates M150 and Q250 came from parts of an extrusion that cooled below 1125°C during the extrusion process. In contrast, the RC series of specimens have relatively uniform microstructures, suggesting that plate R250 came from a section of the extrusion that did not cool below 1125°C during the extrusion process. With regard to the tensile specimens, the uniformity of the microstructure of the ST and RC/D series similarly indicates that plates S40 and R250 came from sections of the extrusion that were maintained >1125°C. However, the fact that one series of tensiles (WE) made from plate N40 was banded and the other (WH) was not indicates that homogeneous and non-homogeneous material can exist in a single plate.

CONCLUSIONS

A comprehensive study of the fabrication metallurgy of the V-4Cr-4Ti alloy has never been undertaken, and consequently, the program is dealing with considerable variations in the microstructures of specimens prepared by different processing paths. Understanding of the kinetics of recovery, recrystallization, and precipitation is incomplete, and we can only speculate on the dynamic interactions occurring during the hot extrusion, particularly since the extrusion temperature is so close to the Ti (OCN) solvus.

The microstructural variations discussed in this report are unlikely to have any major impact on tensile behavior, but the presence or absence of banded microstructures could introduce an anisotropy in crack propagation behavior.

Before any further processing of extruded barstock into plate is undertaken, it would be advisable to undertake a pilot study to investigate the potential benefits of introducing a homogenization treatment at 1150°C to dissolve any Ti (OCN) formed during the extrusion process. Knowledge of the kinetics of recovery, recrystallization, and precipitation needs to be expanded to provide a rational basis for selecting rolling and intermediate annealing schedules that will generate predictable and consistent microstructures.

REFERENCES

1. E. Donahue (UCSB), private communication.

2. D. T. Hoelzer, Fusion Materials Semiannual Progress Report, this volume, pp. 59-63.

3. J. Kurtz, M. L. Hamilton, and H. Li, Fusion Materials Semiannual Progress Report for Period Ending December 31, 1997 (DOE/ER-0313/23), pp. 111-118.

4. R. Petersen, Teledyne Wah Chang, Albany, private communication.